Processing bGeigie Nano log files from car trips

D. M. Wood, June 2020

This tutorial document

- Reviews data of Stone, Whicker, Ibrahim, and Whicker on the ambient dose equivalent [radiation] rate (ADER) along Interstate 70 in Colorado and contrasts it with what can be acquired by a compact, GPS-enabled, data-logging Geiger-Müller unit at highway speeds with samples every 5 seconds.
- Discusses wavelet de-noising and describes in detail the processing of data needed to extract radiation rates and the distance scales over which they vary. Shows how to combine 'there' and 'back' legs for stable numerics.
- Presents simple guidelines for the trade-offs between spatial variation and vehicle speed.
- Compares recently measured with Stone *et al.* data for the Rocky Flats National Wildlife Refuge and its interior, confirming the reliability of the bGeigie Nano for ADER measurements.

Contents

Note: Clicking on a blue link takes you to a somewhere in this document; green links will take you to a Web site or remote document.

Introduction

New capabilities of the SAFECAST QGIS (3.x) version 2 plugin permit more sophisticated analysis of bGeigie Nano log files. In this document I illustrate how I have done some of this. I welcome any corrections or suggestions since I am a relative newcomer to processing such data.

The Front Range of Colorado, by virtue of both altitude and natural soil radionuclides, exhibits the highest background radiation in the United States. This also varies considerably from place to place within the state. The article *Spatial variations in natural background radiation: absorbed dose rates in air in Colorado* by Stone, Whicker, Ibrahim, and Whicker [1], published in 1999, reported 'ambient dose-equivalent [radiation] rate' (ADER) measurements, taken in summer 1995 at 1150 locations in Colorado using a pressurized ionization chamber (PIC). The authors also presented data along Interstate Highways I-25 (north-south) and I-70 (east-west, about 300 locations) with PIC measurements taken at rest every 1-2 km.

"The granites of Colorado's Front Range are particularly enriched in these [radioactive] constituents compared to normal granites…", according to the Stone *et al.*

Such PIC detectors (as can be seen here, Fig. 7 have an essentially flat response to gamma rays over the range of about 70 keV to 10 MeV. The LND 7317 Geiger-Müller tube is not energy compensated, in comparison.

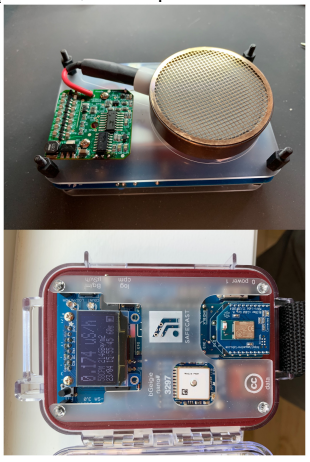

Figure 1: Assembled bGeigie Nano kit. This device was developed by SAFECAST for the measurement of the ADER with this counter orientation. Its calibration was established by SAFECAST (using ^{137}Cs) as 334 counts/m = 1 μSv/hr, permitting ready conversion to the ambient dose equivalent rate.

As discussed elsewhere, the bGeigie Nano is a GPS-enabled pancake Geiger-Müller counter, designed by the SAFECAST project, which acquires data every 5 seconds and logs location, altitude, and count rate to a file. The log file can be post-processed for detailed geographical and radiation rate data. By contrast to the painstakingly acquired precise results of Stone *et al.*, we show here results along I-70 from Arvada to Grand Junction, CO (and back) taken at highway speeds with the counter hanging on the outside of a car window facing outward with its axis horizontal.

With Poisson statistics with count rate N per counting interval one expects relative fluctuations (standard deviation of the mean over the mean) of $1/\sqrt{N}$. In Colorado the mean number of counts per 5 seconds is about 5, so one expects relative fluctuations of $\simeq 1/\sqrt{5} \simeq 0.45 = 45\%$. (The value computed directly is about 50%,

larger because of substantial variation from place to place.) Thus the measured ADER is quite noisy; we discuss the significance below.

Results of Stone et al

We focus here on the the published data along Interstate 70; some will be presented graphically below. General conclusions and remarks include (i) west of the Continental Divide about 60% of the ADER is attributed to terrestrial (soil-based) radiation. East of this the terrestrial fraction rises to about two thirds; (ii) among the 40 communities surveyed along the Front Range the average ADER was 0.143 μGy/h: 0.135 for those below about 2000 m and 0.196 for those above; (iii) about 30% of the observed variation of the ADER is attributable to elevation, partly from elevation and partly because granitic geology (and thus higher soil radiation) is more common at high altitudes and sedimentary geology at lower, and (iv) the 'coefficient of variation' [relative fluctuations in the mean = (standard deviation)/mean] for the terrestrial dose rates was 33%. The authors remark, "The large peak in terrestrial dose rates east of the Continental Divide was primarily responsible for this large CV value." Finally, it is important to note that most data was acquired while the detector was stationary, permitting more careful control over counting statistics.

The 'Continental Divide' separates streams which flow into the Atlantic from those that flow into the Pacific.

Most of their data comes from a sequence of 6 measurements per 1-minute interval Unfortunately, nowhere do the authors report count *rates*, so direct evaluation of statistical noise is difficult since the PIC is automated. They remark, "As mentioned, one of the above locations was also used for a calibration checkpoint where PIC measurements were made over a several-month period. Of the various types of measurements used to check the calibration of the PIC instrument during this period, 56 were unshielded background measurements. For these background measurements, the average percent difference between the means of the six readings in 1 min, and the mean of the 56 dose rates recorded over the 3-mo period was 2.6%. The above results indicate that the mean value of six instantaneous PIC measurements taken over a 1-min period provided a good representation of the true average dose rate at a given sample location." If we attribute *all* of the 2.6% disagreement to Poisson noise, we have $0.026 \simeq \frac{1}{N_{eff}}$, where N_{eff} is the effective number of counts per sampling period, about 1480. Thus we estimate the counts per 1-second interval as about xxxxx. for their typical situations. This is consistent with other published accounts of the use of

My interpretation: each measurement, carried out by pressing a buton, specifies the number of counts in a 1-second sample. There is a 10s interval between such presses, leaving time to record or write down the results. So in 60 seconds there are 10×5s of pauses, 6×1s of measurements, and 4 extra seconds.

bGeigie Nano results

Processing of bGeigie Nano log data

Version 2 of the 'SAFECAST plugin' (developed by OpenGeoLabs at the behest of SÚRO, the Czech National Radiation Protection Institute) is compatible with QGIS version 3.x, an open-source GIS program. The plugin is available from github. It permits graphical trimming of points from a logged trajectory and computes speeds, accumulated distance, and point-by-point and net ADER dose. (This is in addition to QGIS visualization of the trajectory and color-coded ADER values.)

The raw data sets discussed below are available from the SAFECAST repository as bGeigie Import #43182, "Drive along Interstate 70 in Colorado, from Grand Junction to Arvada" and bGeigie Import #47220, "Drive along Interstate 70 in Colorado, from Arvada to Grand Junction". I took care to remove trajectory points corresponding to roadside pauses or a visit to a gas station, and to make the trajectories otherwise as similar as possible, beginning and ending at well-defined points on on-ramps or off-ramps. Despite these precautions, the Grand Junction to Arvada leg (henceforth labeled GJ-A) distance was computed to be 380.9 km, to be compared with 380.6 for the Arvada to Grand Junction leg (A-GJ). It is quite likely that this reflects actual differences in distance along east- and west-bound lanes rather than error in the data, although there are portions of the route with poor GPS coverage (see, for example, the deviation of the trajectory from the west-bound actual lane shown in the margin).

It is customary to decompose the ADER [total = cosmic + terrestrial] into contributions from terrestrial (soil) radiation and from cosmic rays. The latter (and hence the former) is estimated using approximations valid for a wide range of latitudes and altitudes. A number of authors have parameterized this cosmic ray dose rate. We adopted the form of Cinelli *et al.*[2], whereas Stone *et al.* assumed a quadratic dependence:

$$\overset{\circ}{H} = \begin{cases} 27.4\left[0.205\, e^{-1.649z} + 0.795\, e^{+0.452z}\right] & \text{present work} \\ 27.38 + 7\times10^{-6}\, z^2 - 1.2\times10^{-3}\, z & \text{Stone } et\ al \end{cases} \qquad (1)$$

where z is the altitude in m and $\overset{\circ}{H}$ is the ADER in nano Gray per hour (nGy/h). Note that 1000 nGy/h = 1 μGy/h, the units used below. Despite the very different forms assumed the results are very similar over the physical range of altitudes of interest. I have used a relative biological effectiveness of 1 (as for γ rays) in order to convert between grays and sieverts.

on several airplane flights; I read that most passenger jets are pressurized to an equivalent altitude of 2500 meters (8000 feet). I like to hike to about 3600 meters. On the other hand, for those contemplating driving trips at high altitude, this warning (from several sources online):

> Bill Lehnert of LND today verified: "LND 7317-Routine operation at 5000-6000 feet no problem, i.e. Denver, Los Alamos. Above that they work fine until the reverse bow becomes a problem in the housing. Once the bow has reversed, the tube will continue to work fine. It is not a good idea to cycle between high altitude and low altitude, as eventually the seals will suffer."

I verified that the bGN continued to operate normally after the hike to 3600m.

Data acquired occasionally resulted in apparent speeds of zero (especially in tunnels) or real speeds of zero (heavy traffic from the mountains toward Denver on a Sunday afternoon). In cases of a single such point the zero velocity was replaced by its average over adjacent points. For longer sequences, the initial velocity was replicated for all nominally zero values.

These are generally valid for a wide range of latitudes in the northern hemisphere.

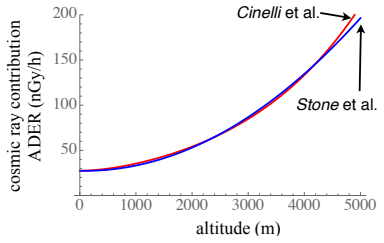

Figure 2: Alternative parameterizations of ADER on altitude don't matter. Only recently did I discover that both sets of authors used the same sea-level (z=0) value.

Dealing with noise in bGeigie Nano radiation results

As noted above, the low mean count rates imply that radiation data will be noisy. There are a number of tactics for 'de-noising' data, but we focus here on two: a simple moving average, and the use of a wavelet transform.

Because of the mean count rates per 5s sampling interval $\overline{n} \simeq 5$ mentioned above, we expect relative fluctuations of $1/\sqrt{5} \simeq 45\%$. A moving average (over say, N points) reduces this to $0.45/\sqrt{N} = 1/\sqrt{\overline{n}N}$.[1] However, there are a couple of drawbacks (of great importance in stock trading, when the relevant data is usually a time series). For our purposes, one is that the dimension of the data array resulting from the moving average has been reduced by (using, say, *Mathematica*) by N-1. This effectively pushes the boundary at which we begin evaluating the 'time series' by 59 time steps. If the signal is time dependent, there is thus a 'lag' in the moving average with respect to the current value at a time t; same for distance in our case.

[1] Thus a moving average over N points is equivalent to multiplying the count rate by N.

For example, for $N = 60$ the first 59 data points are used to compute the moving average evaluated at the 60th point. There are many other options for carrying out moving averages; this is the simplest.

In the context of smoothing bGeigie Nano data with a 5 second sampling interval, this means that a sequence of spatial positions begins a distance something like $(N-1)\times\overline{v}\times 5$ (where $\overline{v}$ is the average initial speed in m/s) from our original origin. In comparing the two 'legs' of a a round trip this requires some care, as discussed below.

On the Grand Junction to Arvada trip the initial speed, averaged over the first 60 points, was 50 km/h, yielding a displacement of 4.1 km.

By contrast, a wavelet transform of a signal concentrates non-noise features into a small number of large-amplitude wavelet coefficients. The choice of threshold for the retained coefficients and a 'refinement scale' determine the extent of de-noising. Although the forward and reverse wavelet transforms are linear, the thresholding is non-linear. The wavelet de-noising process is regarded as *non-parametric*: no particular assumptions need be made about the threshold: there is even a *universal threshold*, adopted here as implemented in *Mathematica*. The *Mathematica* 'module' (subroutine) which accomplishes both the de-noising and elimination of occasionally occurring outliers is shown in Fig. 3 in the margin. Here we adopt a basis of the 'least asymmetric' wavelets of order 7, 6 levels of refinement, and threshold wavelet coefficients using the default *Mathematica* 'Universal' threshold setting. The impact of such choices is discussed in Appendix B.

In a Fourier time-frequency transform one could similarly discard high temporal frequencies to achieve a smooth signal that may or may not be free of noise. One may regard (see this brief tutorial) the wavelet transform for a time-dependent signal as taking us from the time domain to the time *scale* domain. Other useful references [3],[4] provide overviews and the MATLAB examples are helpful.

As an example, Fig. 4 shows part of the data (light blue) from 6000 Poisson-distributed random numbers (mean of 5). In orange is the 100-point moving average result, reducing noise (as verified numerically) by the advertised factor of $\sqrt{100} = 10$. In the lower panel we contrast moving average and wavelet results. It is clear that the wavelet results generally reproduce the principal features of the moving average but are much smoother. The most important

Thresholding methods are discussed in the documentation for the `WaveletThreshold` command. We detect outliers using *Mathematica*'s `AnomalyDetection` command.

De - noise using wavelet transform

```
WavelClean[infile_] :=
 Module[{transform, wavel, hold, detect, outliers, nout},
transform = DiscreteWaveletTransform[infile[[All, 2]],
    SymletWavelet[7], 6];
  transform = WaveletThreshold[transform];
  wavel = InverseWaveletTransform[transform];
  hold = Transpose[{infile[[All, 1]], wavel}];
  (* reconstitute data pairs before outlier detection *);
  detect = AnomalyDetection[hold, PerformanceGoal → "Quality"];
  outliers = FindAnomalies[detect, hold];
  Print[outliers];
  nout = Dimensions[outliers][[1]];
  Print[
   nout
    "obvious outlier data points deleted from wavelet
      denoised data"];
  Complement[hold, outliers]]
```

v 0.9

Warning : because of the stochastic nature of the outlier detection algorithm, the number of detected outliers may differ somewhat from one call to another!

takeaway from this figure is that both the wavelet transform and the moving average agree on structure present in *strictly random data*, which can carry *no physical significance*. This warning holds when interpreting noisy bGeigie Nano radiation data–more work is required to determine which features in a de-noised data set are physically meaningful. An example of the process is given in Appendix C of the document here.

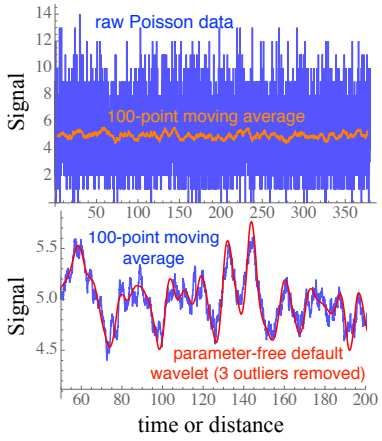

Figure 4: De-noising and smoothing of strictly random numbers. Note close agreement between wavelet [`symlet` order 7, refinement level 6] and moving average results in lower panel, though this has *no physical meaning*.

Comparison of bGeigie Nano results with those of Stone et al.

In Fig. 5 we show the data of Stone *et al.* (top panel) and our data (lower panel). The published figure was digitized and redrawn for flexibility. The upper and lower panels are *not* meant to be in registry– some additional scaling would be required to superpose, for example, altitude features. We note that

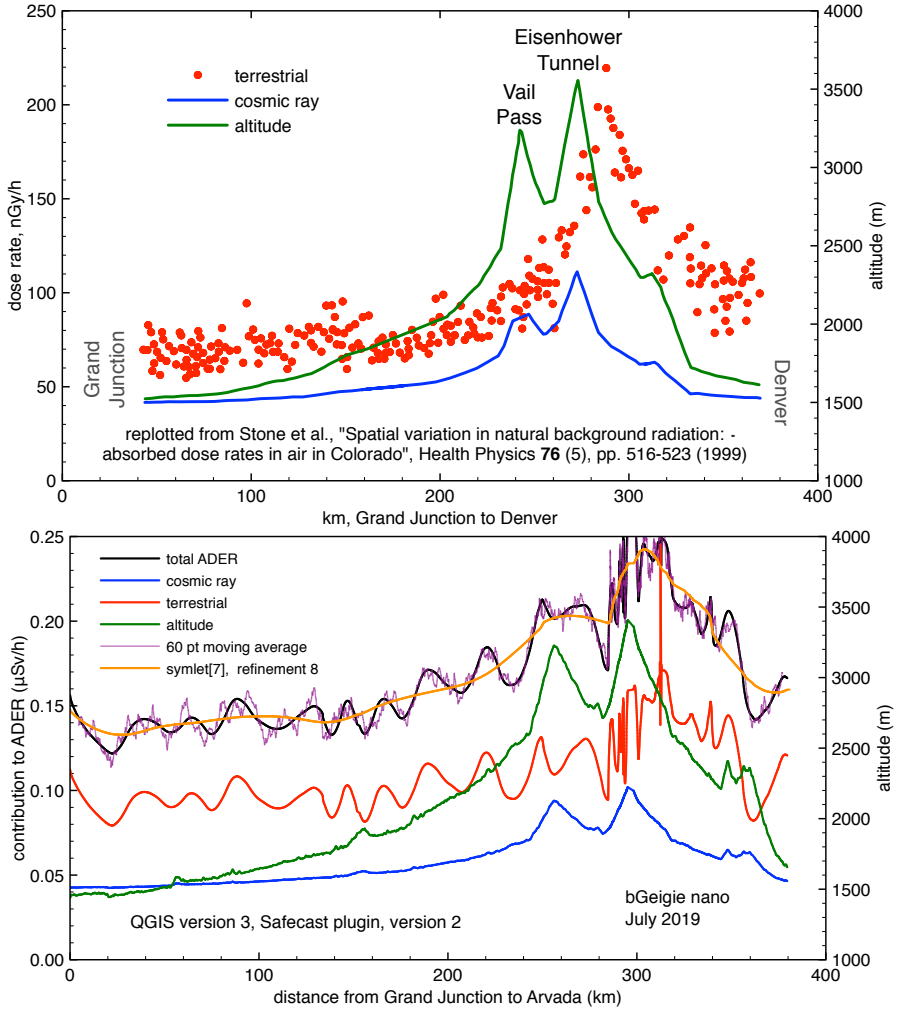

Figure 5: Comparison of 1995 data of Stone *et al.* using a pressurized ionization chamber with de-noised [see text] data acquired in July 2019 using bGeigie Nano Geiger-Müller detector at car speeds. Units are equivalent: 100 nGy/h = 0.1 μSv/h with an assumed relative biological effectiveness of 1 for cosmic rays. Note that the cosmic ray contribution is derived directly from altitude data. A 60-point moving average for total ADER data is shown as a light purple dashed line. Note that peak total ADER occurs east of the Continental Divide (Eisenhower Tunnel). The narrow red peak at around 320 km is an artifact of the wavelet thresholding not detected as an outlier.

1. Superficially the two panels resemble each other quite closely except that a scatter of discrete points has been replaced by a continuous curve for the terrestrial radiation contribution. On the other hand, the average level of terrestrial radiation as measured by the bGN is somewhat higher on the west side of the Continental Divide and somewhat lower near the peak of the ADER.

2. Unsurprisingly, fine details in the relatively slowly varying altitude are evident due to the finer sampling distances made possible by the 5s sampling interval.

3. The amplitude of modulation of the terrestrial component (red) in the lower panel is quite similar to the width of the band of red dots in the upper panel.

4. bGN data approaching the Eisenhower Tunnel is distinctly less smooth than that of Stone *et al.*, possibly reflecting abrupt changes in geology as mostly granitic rock is replaced by sedimentary rock.

We reserve a discussion of whether features evident in the bGN ADER are physically meaningful until after presenting the 'return leg' data.

Combining 'there' and 'back' legs of a round trip

It is worth briefly examining the data acquired during the other leg of the Grand Junction to Arvada trip. Were the endpoints identical and the data acquired in the same way, the various trajectories (*e.g.*, altitude vs. trip distance) should be mirror images. Mathematically,

$$f_{GJ-A}(x) = f_{A-GJ}(D - x) \tag{2}$$

where f are the path functions D is the nominal distance and x the distance along the path from Grand Junction to Arvada: x ranges from 0 to D.

Results can differ for a number of reasons: (i) GPS satellite visibility due to canyon walls, or depending on the time of day of the trips; (ii) especially in Glenwood Canyon the east- and west-bound lanes of I-70 are substantially displaced; (iii) traffic during the GJ-A trip (transit time 5:07:45, 76.3 km/h average speed) was considerably higher than during the A-GJ trip (transit time 4:37:41, average speed 88.7 km/h). (A longer duration will of course result in a higher net computed ADER dose even for identical distances.)

As discussed above, measured and derived radiation quantities suffer from large Poisson fluctuations of the counting rate. As before, we will examine the same two approaches to de-noising: the use of a moving average and a wavelet transform. As above, we adopted a

60-point moving average (in principle, a 5-minute time average in the time domain), and the same set of wavelet parameters used earlier.

Comparing 'there and back' trajectories when using a moving average

A 60-point moving average, as mentioned earlier, causes a time or spatial lag, and modifies the apparent lengths of each leg of the journey, from 380.7 to 377.2 [GJ-A] and from 379.9 to 376.1 [A-GJ], *and* the dimensions of the resulting data arrays. These shifts are quite comparable to our earlier crude estimate of 4.1 km. Measured features are tied to the *actual* location, not that resulting from the moving average. For this reason the quantity D on the right side of Eq. (2) was replaced by D+δ, where δ is meant to 'soak up' most of the impact of the truncation of the range due to the moving average. The mean square difference of

$$\Delta = \int_a^b dx \left[f_{GJ-A}(x) - f_{A-GJ}(D + \delta - x) \right]^2 \qquad (3)$$

where a and b are selected to be 5 and 375 km, respectively, to assure that interpolation is well defined for both legs.

Fig. 6 shows the quantity Δ for both the total measured ADR (in blue), and for the altitude (in green), as a function of the shift δ. It is worth noting that (i) the value of the shift δ is similar to the truncations in leg length due to the moving average construct; (ii) the value of δ ($\simeq$ 3.5 km) which minimizes the there/back difference is the same for the altitude profile as for the ADER profile. In Fig. 7 we compare the 60-point moving average for the altitude (which does not suffer from Poisson noise, upper panel) and the ADER, which remains jagged despite reasonable agreement between the two legs.

Comparing 'there and back' wavelet de-noised trajectories

As earlier noted, apart from its parameter-free removal of a great deal of Poisson noise, the wavelet approach (since it re-synthesizes the de-noised dateset) does not change the length of the spatial region (or total time duration) of the sample. Thus no special measures need to be take to 'invert' the trajectory. Results analogous to those for the moving average are shown in Fig. 8, as above using `symlets` of order 7 and refinement level 6.

Careful inspection of the altitude curves display much finer detail present in both legs of the trip. On the other hand, the same disagreements (although much smoother) are present in the ADER curve as we saw in the moving average curve.

As warned above, features which are entirely random in origin may persist through a moving average, as discussed in detail here.

Precisely which features survive this moving average to be physically meaningful requires more analysis, such as that here.

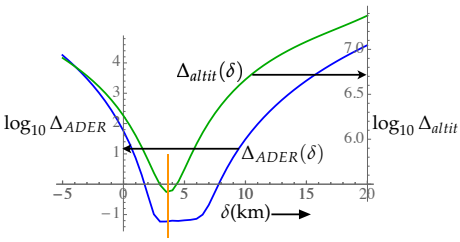

Figure 6: A measure of the 60 point moving average-induced shift between the 'forward' and 'back' legs of the trip, for the altitude (green) and ADER (blue). Note that the difference is minimized for both scenarios for a shift of about 3.5 km.

It is easy to define a continuous function of x by simple interpolation using *Mathematica* via `f(x) = Interpolation[arvtogj][x]` where `arvtogj` is the array of x-y data pairs of interest. These are the functions used in Eq. 3.

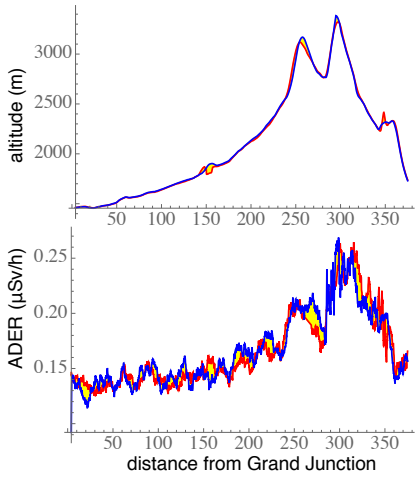

Figure 7: Superimposed moving average curves for trajectory from Grand Junction to Arvada (red curves) and from Arvada to Grand Junction (blue curves). The region between the two (the difference) is highlighted in yellow. Upper panel: altitude; lower: measured ADER.

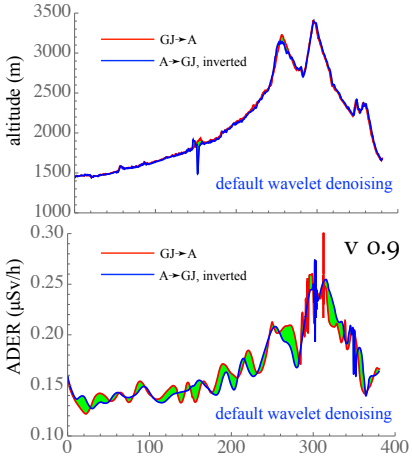

However, comparison of the 'forward' and 'back' curves permits identification of common features that are thus less likely to be due to statistical noise alone. In comparing red and blue curves for the ADER we note

1. The amplitude of red and blue curves is generally quite similar in each region of the trajectory. The precise alignment of the curves for the altitude data allows us to conclude that the red and blue ADER curves must be dominated by statistical noise, making it more difficult to attribute structure in the curve to geological features. (This is addressed further below.)

2. Large features beyond 225 km from Grand Junction are reasonably consistent between the two trajectories; below 225 km or so there appear to be weaker correlations between the two curves.

Quick overview of measured ADER within the Rocky Flats National Wildlife Refuge

[This topic is primarily about the *reliability* of the bGeigie Nano's ADER measurements, not about geo-tagging *per se*.] Stone *et al.* noted, "Land adjacent to the Rocky Flats Environmental Technology Site [now the Rocky Flats National Wildlife Refuge and the DOE-controlled 'central operable unit' (COU)] was included in this portion of the study. No measurement anomalies were detected around the site and, therefore, PIC readings appear to reflect normal total background values for the area (130-147 nGy h-1)."

The same bGeigie Nano was used to map radiation levels (at walking speed) on trails inside the Refuge in April, and within the COU (by car and on foot) in June of 2019. Histogram results are shown in Fig. 9. On the trails the ADER was measured to be 0.1397 ± 0.0006 μSv/h and within the COU, 0.1395 ± 0.0018 (where the ± indicates 95% confidence interval). The average of the range quoted by Stone *et al* is 0.1385, so the more recently measured values are entirely consistent.

These comparisons may shed some light on the reliability of the bGeigie Nano for routine measurement of the ADER under a variety of geological and altitude conditions.

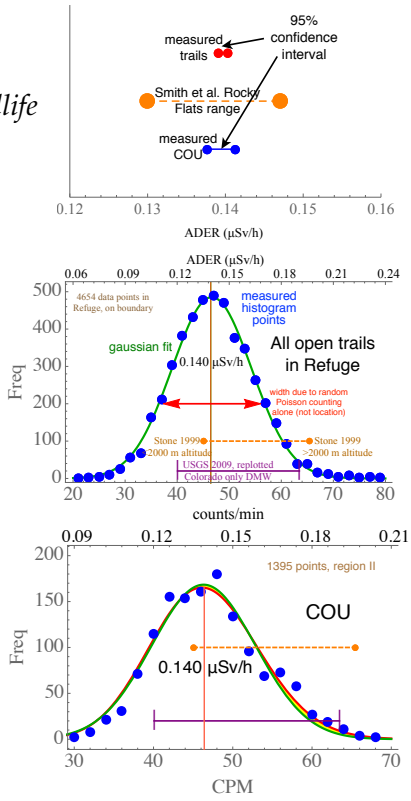

Figure 9: Data for bGeigie Nano surveys or trails within the Rocky Flats National Wildlife Refuge and the COU.

Spatial resolution of data acquired in a moving car

Neither wavelet transform nor moving average results provide a direct estimate of the length scales over which we can trust deduced variations in radiation-related quantities. Ultimately, the best indication that such features exist in the data presented so far is the 'there

and back' comparisons along I-70, since we expect partial cancellation of random noise. As we have seen above [for example, the light purple curve in the lower panel of Fig. 5 or the lower panel in Fig. 7], the moving average process produces jagged fine-scale features which are probably not physically relevant. We are thus left with the (`symlet` order 7, refinementn level 6) wavelet de-noised curves as the most reliable and convenient representation of spatial variations.

Before turning to an analysis, it is useful to briefly examine other measured or deduced quantities which bear on this. Fig. 10 shows medium- and fine-scale variations of the wavelet-smoothed ADER, the car speed, and the horizontal dilution of precision (HDOP) reported by the bGeigie Nano log. It is tempting to ascribe the 'hiccup' in the wavelet-de-noised ADER curve at about 300 km into the trip to the poor (high) HDOP, although the speed curve indicates stop-and-go traffic around this time as well.

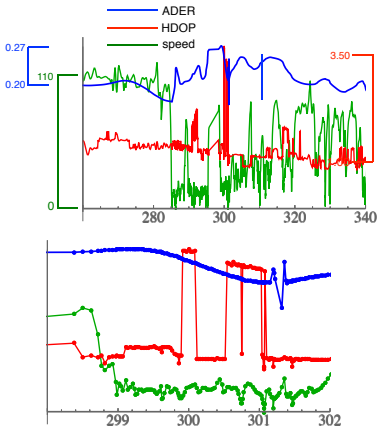

Figure 10: Medium-scale (top) and fine-scale (bottom) variation of the measured, de-noised ADER (blue), the de-noised car speed (green), and the HDOP (red) during the Grand Junction to Arvada leg. Colored brackets indicate minimum and maximum values for each curve.
These hiccups/discontinuities in wavelet inverse transform have been reported to Wolfram as a bug.

Trade-off between resolution and Poisson fluctuations

As mentioned previously, for a Poisson distribution of mean count rate $\mu = \overline{n}$, the relative counting fluctuations (or relative uncertainty in the mean count rate)

$$\delta n \equiv \frac{\sqrt{\overline{(n-\overline{n})^2}}}{\overline{n}} = \frac{\sqrt{\overline{n^2}-\overline{n}^2}}{\overline{n}} = \frac{\sqrt{\mu}}{\mu} = 1/\sqrt{\mu} = 1/\sqrt{\overline{n}} \qquad (4)$$

Warning: this expression tacitly assumes a specified sampling interval! If the sampling interval is 5 seconds and the mean count per sampling interval is 4.175 we would find $\delta n \simeq 0.489$. If we changed the sampling interval to 60s the mean count per sampling interval would change to 12×4.175=50.1 and the relative uncertainty δn would drop by a factor of $1/\sqrt{12}$ to $1/\sqrt{50.1}$ = 0.141. Thus we can achieve a much higher mean count rate (and thus a smaller relative uncertainty) simply by making our effective 'sampling time' much longer than 5s. For a moving vehicle this goes hand in hand with a larger distance between samples. Thus we expect a tradeoff between smaller statistical uncertainty and coarser spatial resolution.

These count rates are selected to yield an ADER of 0.15μSv/h, comparable to values along I-70 apart from the Front Range, given 334 counts/min = 1μSv/h.

If the average count rate (physically determined by radiation levels) is $\overline{p}$ per second and we want a particular value of relative uncertainty δn we would thus need to count for a time T (in s) satisfying $N_{count} = \overline{p}T = \overline{n} = 1/(\delta n)^2$. During this time a car moving at speed v would have moved a distance $\Delta x = vT$. With v measured in km/h and $\overline{p}$ in counts/s, the car would have moved a distance $\Delta x = v/\left(3.6\,\overline{p}\,(\delta n)^2\right)$ meters.

By contrast, during the 5s sampling interval of the bGeigie Nano the car moves $5v/3.6$ meters. We adopt a typical speed of 80 km/h

for concreteness. Then the 'intrinsic' resolution of car measurements (the distance moved between 5s samples) is about .111 km, well above the assumed GPS measurement error of a few meters. On the other hand, if we require relative statistical fluctuations of only 10%, we would have traveled a distance of 2.22 km to achieve the required total number of counts. We can in principle achieve this simply by performing a moving average of length $2.22/0.11 \simeq 20$, since we confirmed above [footnote 1] that such a moving average effectively increases the number of counts by this factor.

Fourier analysis

The issue of which measured spatial variations in radiation rates from a moving vehicle are *reliable* is somewhat complicated. Obviously the distance over which a car moves in one sampling interval (5s) sets a highest spatial frequency (shortest distance), provided it is much more than the GPS horizontal position uncertainty. However, the low count rate due to background levels of radiation (in Colorado, about 5 counts per 5s) forces us to consider a coarser length scale, over which variations in the measured ADER are *not* dominated by Poisson counting noise. We approach this in a roundabout way, using wavelet de-noised ADER data *then* carrying out a discrete Fourier transform. We examine the power spectrum to identify a reasonable 'range'.

Results of a discrete Fourier transform of the measured and de-noised ADER over a 12 km portion of trails (traversed on foot) within the Rocky Flats National Wildlife Refuge in Arvada, CO are shown in Fig. 11. The upper panel shows that the lowest 25 Fourier components really do dominate the power spectrum, while the lower shows that these alone roughly reproduce trends. We can roughly estimate the highest important spatial Fourier component via

$$k_{max} \simeq n_c \times 2\pi/L \tag{5}$$

where L is the length of the trip and we recognize $2\pi/L$ as the 'fundamental' spatial frequency. Thus n_c is the cutoff 'overtone' above which higher Fourier components may be approximately neglected. Using $n_c \simeq 24$, this suggests a spatial resolution of something like $2\pi/k_{max} = L/n_c \simeq 0.5$ km. (In other words: the distance between adjacent local maxima and local minima in the smoothed curve is about 0.5 km: there are about 28 maxima or minima over a distance of 12 km from inspection of the smoothed ADER.)

We may in turn use this number to estimate how many *counts* were acquired over this distance. This will provide insight into the Poisson noise levels *below which* we can possibly trust the wavelet de-

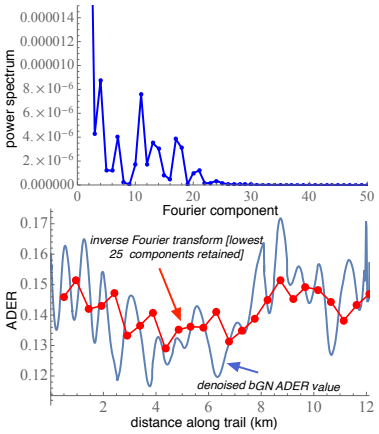

Figure 11: Fourier analysis of ADER data along southern trails in the Rocky Flats National Wildlife Refuge. Upper panel shows power spectrum of discrete Fourier transform, lower panel the inverse Fourier transform using lowest 25 Fourier components.

There are approximately as many loops (half-periods of oscillation) in the smoothed ADER as there are appreciable components in the transform. We are thus using the Fourier transform mostly to formalize this relationship.

This does *not* mean that finer-scale detail does not exist, but that the de-noising or smoothing process needed to get rid of large Poisson noise forces this length scale on us.

noising to detect a signal. Using the bGeigie Nano calibration of 334 counts/m = 1μSv/h, since the average speed was 4.1 km/h and the average ADER was 0.141 μSv/h:

$$\begin{aligned} N_{count} &\simeq 0.50\text{km}/(4.1\text{km/h}) \times 60\text{min/h} \quad [\text{minutes}] \\ &\quad \times 0.141\mu\text{Sv/h} \times [334 \text{ counts/min}]\,/(1\mu\text{Sv/h}) \\ &= 345 \end{aligned} \tag{6}$$

The Poisson relative uncertainty $1/\sqrt{N_{\text{count}}}$ is thus about 5.4%.

We may use the much longer highway trips discussed above to provide two more estimates at a very different acquisition speeds. For the Grand Junction to Arvada leg of this trip we show in Fig. 12 the power spectrum of the discrete Fourier transform, (top panel), the lowest 50 Fourier components (middle panel) [blue = GJ-A, red = A-GJ]. In the lowest panel is shown (blue curve) the wavelet de-noised ADER during the trip (with its maxima shown as magenta dots for ease in counting features), and the discrete inverse Fourier transform. Small red dots show the real part and green large dots show the modulus of the inverse transform, demonstrating that the imaginary part is a small fraction of the total. While the inverse transform only approximately resembles the ADER curve, trends are reproduced and the number of peaks and valleys is very similar.

It is clear that the power spectrum is dominated by the lowest 40 Fourier components (in blue, the Grand Junction to Arvada leg, in red the other leg). Truncating the Fourier analysis to the lowest 40 components, the inverse Fourier transform approximately reproduces the ADER curve: the real part of the inverse as small red dots, the modulus as larger green dots. Peaks in the ADER curve are indicated as magenta dots to facilitate feature counting. For the GJ-A trip $n_c \simeq 37$, while the A-GJ trip exhibits $n_c \simeq 32$. We summarize the data for these three 'sample trips' at very different acquisition speeds and distances in the Table below, which used data directly from the QGIS SAFECAST plugin statistics panel.

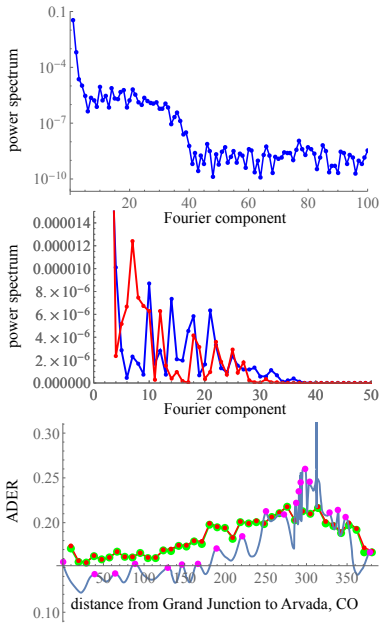

Figure 12: For Grand Junction to Arvada trip, power spectrum of discrete Fourier transform of de-noised ADER data, top two panels, and inverse Fourier transform compared with de-noised data. In middle panel we show results for this trip in blue, with the Arvada to Grand Junction trip shown in red.

case	L	$\overline{v}$	$\overline{\text{ADER}}$	n_c	D_{FT}	counts	RU
RF trails	12.1	4.1	0.141	24	0.5	347	0.054
GJ→A	381.	74.4	0.183	37	10.3	508	0.044
A→GJ	381.	82.8	0.169	32	11.9	487	.045

Table 1: Trip length L in km, average speed $\overline{v}$ in km/h, average ADER in μSv/h, characteristic length D_{FT} estimated from Fourier transform in km. Other quantities [RU = relative uncertainty in counts] are dimensionless. Rounded from higher-precision calculations.

Perhaps the most interesting result from these estimates is that the number of counts over the estimated range D_{FT} is roughly a constant, say 500. This suggests that the features in the de-noised data emerge when the relative uncertainty in the number of counts is at or below about 5%. We also note that the ratio $D_{FT}/\overline{v}$ is approximately constant.

The GJ→A deduced counts are higher because the average ADER is larger (longer trip time–heavier traffic) and the average speed is lower (same reason).

Simple model based on de-noised data distance scales

Above we crudely assessed the number of counts (about 500) needed to account for the spatial signals observed in three different trip trajectories. The working assumption is that this number is large enough to permit the 'structure' to be discernible over Poisson noise.

As discussed above, the relative fluctuations (relative uncertainty) in the counting rate for a Poisson process of mean count rate $\overline{n}$ is

$$(\Delta n)\,/\overline{n} = \sqrt{\overline{n}}/\overline{n} = 1/\sqrt{\overline{n}}, \tag{7}$$

about $1/\sqrt{5} \simeq 0.45$ for an average count rate of about 5 per 5s, as in the data above. However, we have seen that by requiring a *larger* number of counts (the 500 above) it is possible to detect features in the de-noised ADER profile for a trip. The relative uncertainty in the number of counts has then dropped to about $10\times$ smaller than the 0.45 of the 5s count rate.

As discussed above,

$$N_{count} \simeq D \times \frac{1}{\overline{v}} \times 60 \times \overline{ADER} \times 334, \tag{8}$$

or $D \simeq 0.0250\ \overline{v}/\overline{ADER}$.

In Fig. 13 we show a contour plot of the characteristic distance scale D as a function of the vehicle speed (x axis) in km/h and a logarithmic ADER scale (y axis) measured in μSv/h, and with log-log scales for ease of reading low speed values, lower panel. Obviously measurements taken at at very low speeds are capable of fine spatial resolution (limited by GPS errors) while only distances of tens of km are readily detectable at highway speeds and background-level radiation. The dashed red (orange) line indicates values for A→GJ (RF trails).

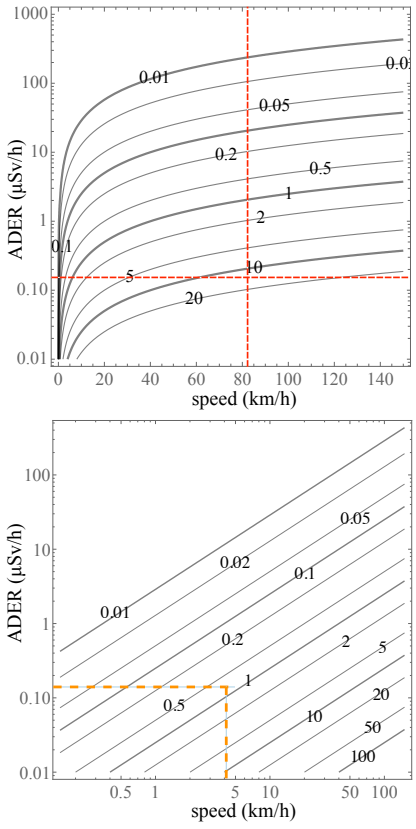

Figure 13: Contours of constant distance scale D which can be probably be detected in wavelet de-noised bGeigie Nano data as a function of vehicle speed and radiation rate (ADER). Dashed lines indicate examples from Table.

Quick examination of data from a signal to noise perspective

If we denote the local value of the counts per sampling time as $R(x)$, how large and abrupt must the variations in $R(x)$ be in order to be detectable in the de-noised data? In Appendix B we show a model that indicates that (i) we should define the signal to noise ratio from $R(x)$ via

$$[\mathrm{S/N}](x) = \frac{\left|R(x) - \overline{R}\right|}{\sqrt{\overline{R}}} \tag{9}$$

and (ii) the S/N ratio should exceed about 0.15 to be detectable. The numerator is the 'excess count rate' (above the mean rate) and the denominator is the 'noise' due to Poisson fluctuations, which we identify as standard deviation of the background Poisson count rate. We could in principle replace the numerator by the square root of the

mean square fluctuations in the count rate about the mean at location x.

This is an extraordinarily naive analysis. Nonetheless, we can at least verify that it is *consistent* with already discussed data. If we revisit the data shown in Fig.11 we see variations in the ADER from about 0.12 to 0.17, with an average of about 0.14. Translating this into counts [per minute] so as to preserve a dimensionless signal/noise ratio, we find the numerator ranges from

Conclusions

1. The bGeigie Nano at highway speeds, in conjunction with the version 2 SAFECAST QGIS plugin, yields precise and reproducible altitude profiles.

2. At highway speeds radiation profiles require careful de-noising. Of the two methods of de-noising used (a moving average or a wavelet transform) the wavelet transform appears much more effective than the moving average.

3. By simple Fourier analysis we identified an approximate distance scale D large enough for the 'signal' to sufficiently dominate the 'noise' due to Poisson fluctuations in the presence of background radiation. It appears that about 400-500 counts (over the distance D) are required for the wavelet de-noising to detect spatial fluctuations in the ADER. This roughly constant value permitted a simple model to be used to estimate the dependence of this distance on the radiation rate and vehicle speed.

Open questions

At this point there remain a number of questions when analyzing a bGeigie Nano (or other) data log.

If we denote the local value of the ADER as $R(x)$, how large and abrupt do the variations in $R(x)$ need to be in order to be detectable in the de-noised ADER data? Is there a critical 'signal to noise' ratio guaranteeing that a feature corresponds to physical reality (or will be detectable)?

There is no 'signal' (in a signal+noise view) without inhomogeneity of the radiation levels. Thus we need to consider how to classify this inhomogeneity. The bGeigie Nano data log is time series data with (almost perfectly) uniform time steps. After processing (such as de-noising) the ADER vs. distance data can continue to be treated as some sort of fictitious 'time series' with non-uniform steps (due to non-uniform speed). It is possible that the sophisticated tools of

time series analysis can be applied to bGN logs either before or after processing to clarify the questions above.

In the Appendix is a model for a non-uniform radiation-distance trajectory which

Acknowledgments

Thanks to Kim Griffiths, who dutifully carried the bGeigie Nano around the Central Operable Unit of Rocky Flats in June 2019, and to Bill Schmitz, who assisted in setting it up on a car window from Arvada to Grand Junction and back, and indulged my idiosyncrasies in July 2019.

Appendix A: Choice of wavelet order and refinement level for ADER de-noising

Since we have no special expectations about the shape of ADER peaks along paths, we have selected the set of 'least antisymmetric' orthogonal wavelets, often referred to as `symlets`. Using these, we find that the variation of de-noising results with the order (first index) is quite mild (as it is increased cusps disappear and curves become smoother), so we have selected symlets of 7th order. Results for the de-noised GJ-A ADER data as the 'refinement level' r varies from 2 to 4 are shown in the upper panel of Fig. **??**. The lower panel shows results for r=5,6,7. It is clear that the scale expands with r. As a consequence, the value of r has a strong impact on the number of oscillations (and to some extent, the amplitude) of the resulting de-noised curve. A significant fraction of wavelet transforms suffer from (so far) unexplained 'glitches' (abrupt almost vertical lines, corresponding to a number of data points at the same 'distance' but spanning a large vertical range.

It is clear that the choice of wavelet refinement level is a very powerful tool in denoising radiation counting data. Too low and the data remains noisy, too high and the curve is so smooth that important details may be lost. As a compromise, all de-noising in the text was carried out with 7th order `symlets` and a refinement level of 6.

Appendix B: Crude model for detectable changes in the ADER

How small a difference in radiation rates *could* we detect in the presence of a given level of Poisson noise in our data?

As a model, we consider a change in count rate (say, per minute)

along a one-dimensional path of the form

$$n(x) = n_0 + \Delta \times \quad 2\left(\frac{1}{1+e^{(x-x_2)/L}} - \frac{1}{1+e^{(x-x_1)/L}}\right) \qquad (10)$$

where x is the location along our path. Here n_0 is the original (background) count rate and Δ is the difference at the peak of the 'envelope' function (which multiplies Δ). The envelope function is picked to go smoothly to zero to the left of x_1 and to the right of x_2; the distance L determines how abruptly the envelope approaches zero. Then we generate a large number of random numbers from a Poisson distribution of mean $n(x)$, de-noise this list using the wavelet transform we have previously discussed, and decide whether the de-noised count rate curve tracks the envelope function well enough for us to detect.

We might *expect* the relevant quantity to be the ratio Δ/n_0, which we call the *contrast* of the spatial change in count rate. But in fact it is the *signal to noise* ratio

$$\mathrm{S/N} = \Delta/\sqrt{n_0} \qquad (11)$$

which determines 'visibility'. The difference matters because the level of Poisson noise is determined by the square root of its mean. In Fig. 14 we make several points.

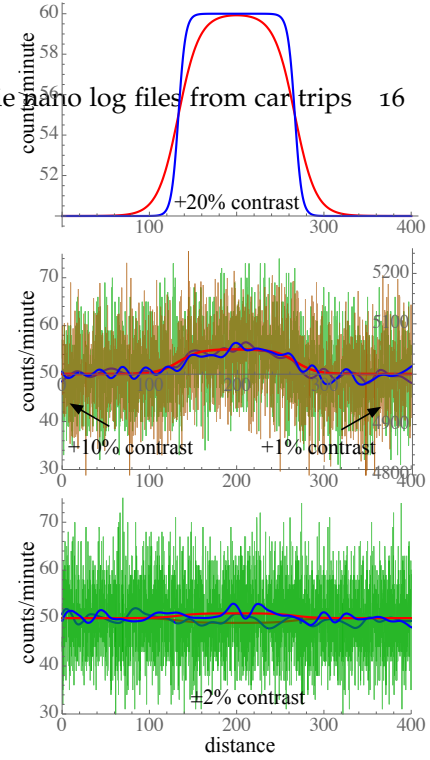

Figure 14: Envelope function with two different settings of parameter L, top panel. Middle panel:10% contrast at 50 counts/minute (left axis) compared with 1% contrast at 5000 counts/minute (right axis). De-noised curves are shown in blue; they are very similar because the signal to noise ratio (not the contrast) is identical for the two cases. Bottom panel: demonstration that a 2% contrast is marginally detectable, suggesting a minimal signal/noise ratio of about 0.15.

1. The parameterization of the path can be made abrupt or very smooth. Such changes in the model might probe the sensivity of the wavelet transform, expected to be very robust under such changes.

2. It is in fact the signal/noise ratio that determines visibility of changes in the count rate. The left and right axes of the middle panel are for $n_0 = 50$ and $n_0 = 5000$ with $\Delta = 5$ and $\Delta = 50$, respectively. The contrasts are very different (10% and 1%, respectively) but the signal/noise ratios are identical.

3. Using a count rate per minute typical of Colorado, we see that 2% changes in contrast might be marginally detected. This amounts to a lower signal/noise ratio of about 0.15.

Appendix C: Statistics without a statistics course

The terminology of statistics is sometimes confusing and frequently not uniform across users. We envision a measurement on a system, for example the writing down the number of counts of a radiation detector in a specified interval (say, 1 second). We would like to specify the average (or 'mean') number of counts per interval and some measure of how uncertain we are about this value. Obviously if we

make only one meausurement we can *assume* the number of counts is 'representative', but to quantify this we must make a similar measurement several more times.

1. The *operations* ('mean', 'standard deviation", etc.) have meaning for as few two data points, but the *theory* of statistics generally applies in a situation where the number of measurements (or data points) becomes very large ($\gg 1$, meaning much larger than 1).

2. We happen to know that radiation counting is described by the 'Poisson distribution', which holds when the probability p of a particular nucleus decaying (and thus emitting a gamma ray, for example) in our count interval is completely random and extraordinarily tiny ($\ll 1$, say 10^{-12}) but the number N_n of such nuclei is very large ($\gg 1$, say 10^{13}) in such a way that $N_n p$ is finite (say, about 10).

What can we say about how the average (mean) count rate changes with the number of measurements, and the uncertainty

Rather than using the formalism of statistics, the examples below are strictly numerical, imitating as closely as possible the task someone carrying out measurements with only rudimentary knowledge of Poisson statistics would face.

Fig. **??** shows two sequences of measurements taken on a system which shows about 50 counts per minute. In each sequence we measure the count rate over 100 minutes, taking one measurement per minute. Q: Which sequence is more reliable? A: The two are exactly as reliable! It is only in the limit of

How uncertain is the mean I compute from 5 measurements

How uncertain is the mean I compute from 5 measurements, but repeated many times? This we *can* answer

How much better are 10 measurements than 5 measurements? By inspecting Fig. **??**it is fairly clear that we cannot meaningfully quantify this if we make *only* 1 set of 10 measurements. H

References

[1] J Stone et al. "Spatial variations in natural background radiation: absorbed dose rates in air in Colorado". In: *Health Physics* 76.5 (1999), pp. 516–523.

[2] Giorgia Cinelli et al. "European annual cosmic-ray dose: Estimation of population exposure". In: *Journal of Maps* 13.2 (2017), pp. 812–821. ISSN: 17445647. DOI: 10.1080/17445647.2017.1384934.

[3] Amara Graps. "An Introduction to Wavelets". In: *IEEE Computational Science and Engineering* 2.2 (1995), pp. 50–61. ISSN: 10709924. DOI: 10.1109/99.388960.

[4] William T Vetterling et al. *Numerical Recipes in F77*. 1992, pp. 644–649. ISBN: 052143064X. URL: papers3://publication/uuid/42C52282-20B5-4159-9E1B-2E89F2631AAA.